Supplement for

The optical properties and in-situ observational evidence for the formation of brown carbon in cloud

Ziyong Guo[1,2,3], Yuxiang Yang[1,2,3], Xiaodong Hu[1,2,3], Xiaocong Peng[1,2,3], Yuzhen Fu[1,2,3], Wei Sun[1,2,3], Guohua Zhang[1,3,4], Duohong Chen[5], Xinhui Bi[1,3,4], Xinming Wang[1,3,4], Ping'an Peng[1,3,4]

[1] State Key Laboratory of Organic Geochemistry and Guangdong Key Laboratory of Environmental Protection and Resources Utilization, Guangzhou Institute of Geochemistry, Chinese Academy of Sciences, Guangzhou 510640, PR China

[2] University of Chinese Academy of Sciences, Beijing 100049, PR China

[3] CAS Center for Excellence in Deep Earth Science, Guangzhou, 510640, China

[4] Guangdong-Hong Kong-Macao Joint Laboratory for Environmental Pollution and Control, Guangzhou Institute of Geochemistry, Chinese Academy of Sciences, Guangzhou 510640, PR China

[5] State Environmental Protection Key Laboratory of Regional Air Quality Monitoring, Guangdong Environmental Monitoring Center, Guangzhou 510308, P. R. China

Correspondence to: Guohua Zhang (zhanggh@gig.ac.cn)

Text S1. Method

EEMs

The scanning range of excitation (Ex) and emission (Em) was 200-500 nm and 200-600 nm, with the wavelength increments for Ex and Em at 5 and 1 nm, respectively. The band-passes for Ex and Em were set to 10 nm. The relative contribution ratio of chromophores in the sample was estimated by using the maximum fluorescence intensity (F_{max}) of chromophore (Chen et al., 2016). The fluorescence index (FI), recent autochthonous contribution (BIX), and humification index (HIX) can be calculated by the ratio of fluorescence intensity at Ex/Em of 370/470 nm to 370/520 nm, Ex/Em of 310/380 nm to 310/430 nm, and at Ex/Em of 255/434-480 nm to 255/300-344 nm (average intensity over the wavelength), respectively (Chen et al., 2016). These indexes may indicate whether DOM is contributed by the terrestrial and microbial sources (FI) (McKnight et al., 2001), autochthonous or biological sources (BIX) (Huguet et al., 2009), or estimate the degree of maturation of DOM (HIX) (Zsolnay et al., 1999).

PMF analysis

PMF solutions of 2-5 factors were analyzed and showed the convergence result, and the Q value and Q_{robust}/Q_{theory} were shown in table S3. Finally, the 3-factor solution was selected as the best source analysis result because the Abs_{365} would become an independent factor when 4-5 factors were analyzed, which was lack of physical means. The bootstrap on the 3-factor solution showed a stable result, with >85 out of 100 bootstrap factors mapped with the based run, and when Fpeak was equal to 0, the Q value showed a result best.

Underestimated of cloud droplets

The collect size of GCVI and cloud water collector was 7.5 and 3.5 μm, respectively, which might cause the underestimated of WIOC, which could be estimated using follow equation:

$$Percent = 100 \times \left(\frac{Abs_{370,WS-BrC}}{Abs_{370,total-BrC}} - \frac{Abs_{370,WS-BrC}}{Abs_{370,total-BrC} \div (1 - underrstimated)}\right)$$

Where, $Abs_{370,WS-BrC}$ is the light-absorption coefficient of cloud water, $Abs_{370,total-BrC}$ is the light-absorption coefficient of cloud RES particles that calculated from AE-33 data. If we assume that GCVI missed 30% of cloud droplets, it will lead to an underestimate of about 16%.

SNA (sulfate, nitrate and ammonium)

SNA was calculated by using follow equation:

$$SNA = C_{NO_3^-} + C_{NH_4^+} + C_{SO_4^{2-}}$$

Where $C_{NO_3^-}$,$C_{NH_4^+}$,and $C_{SO_4^{2-}}$ were concentration ($\mu g \cdot m^{-3}$) of NO_3^-, NH_4^+, and SO_4^{2-}, respectively.

Refractive index calculation

The extinction ability of atmospheric aerosol can be characterized by the refractive index ($m = n + ik$), which is a complex number, where the imaginary part (k) is caused by light-absorption of aerosol, and can be calculated by the following equation (Gelencsér et al., 2003):

$$k = \ln 10 \times \frac{A_\lambda \times \lambda}{4\pi \times L}$$

Where A_λ is the absorbance of cloud water, λ is the wavelength, and L is the cuvette path length (0.01 m).

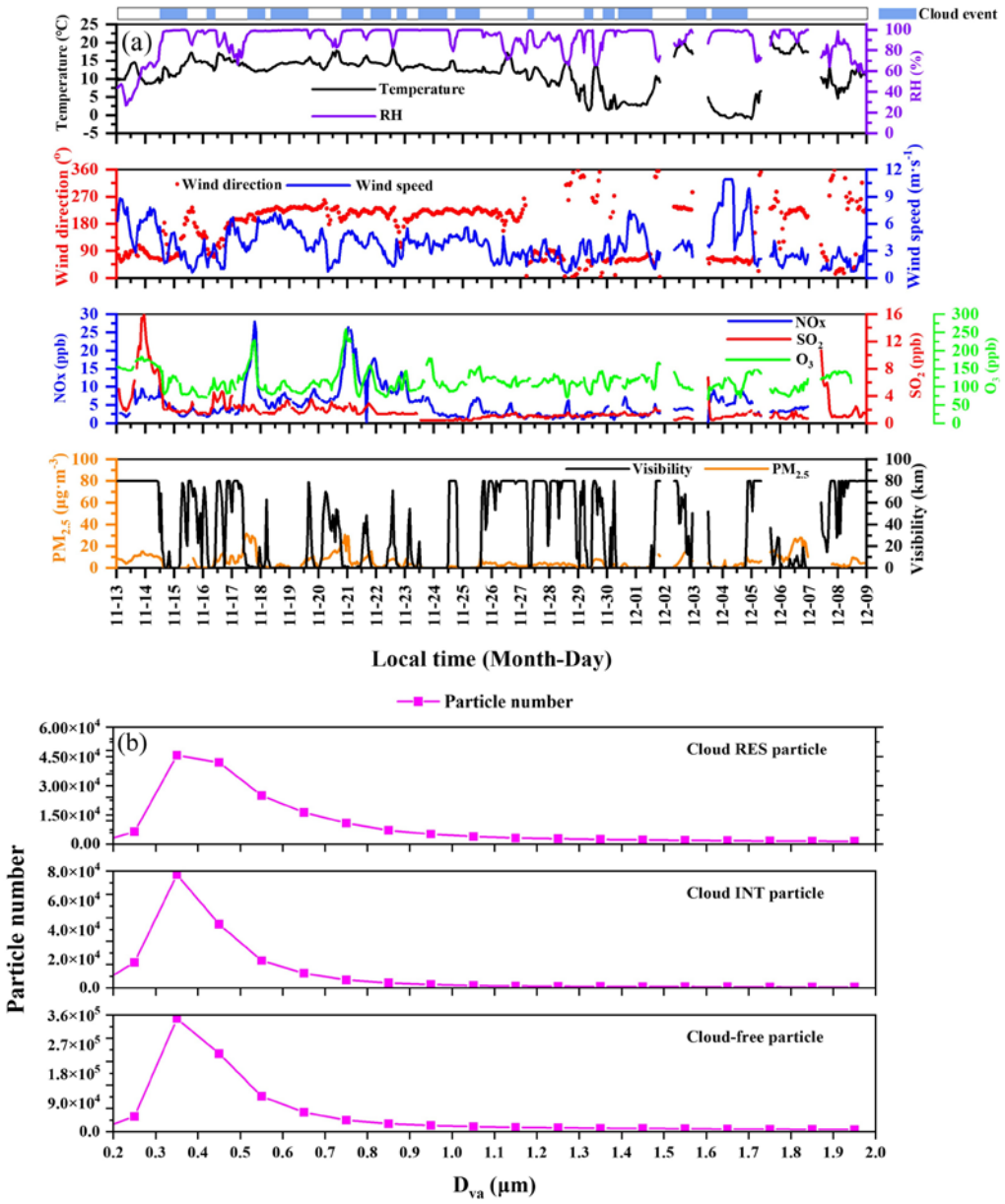

Figure S1. (a) The meteorological parameters such as temperature (℃), RH (%), wind direction (°) and speed ($m \cdot s^{-1}$), NOx (ppb), SO_2 (ppb), O_3 (ppb), $PM_{2.5}$ ($\mu g \cdot m^{-3}$), visibility (km) during field observation, and (b) size distribution of cloud RES, cloud INT, and cloud-free particles.

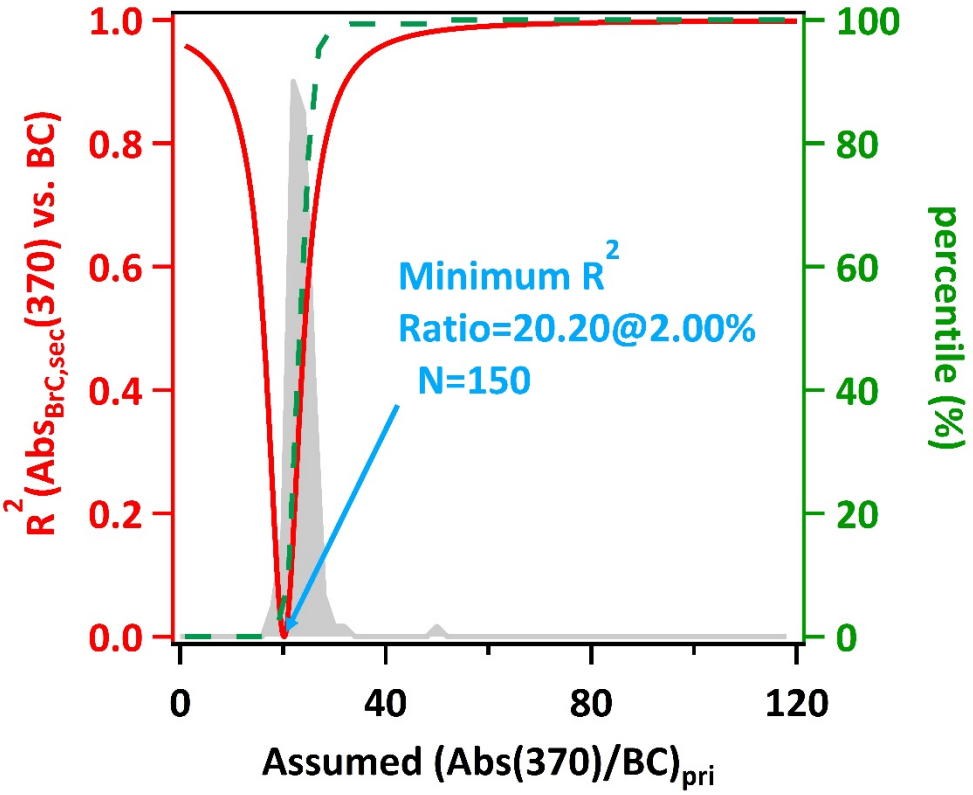

Figure S2. Illustration of the minimum R squared method (MRS) to determine the light-absorption of primary and secondary BrC in the cloud RES particle.

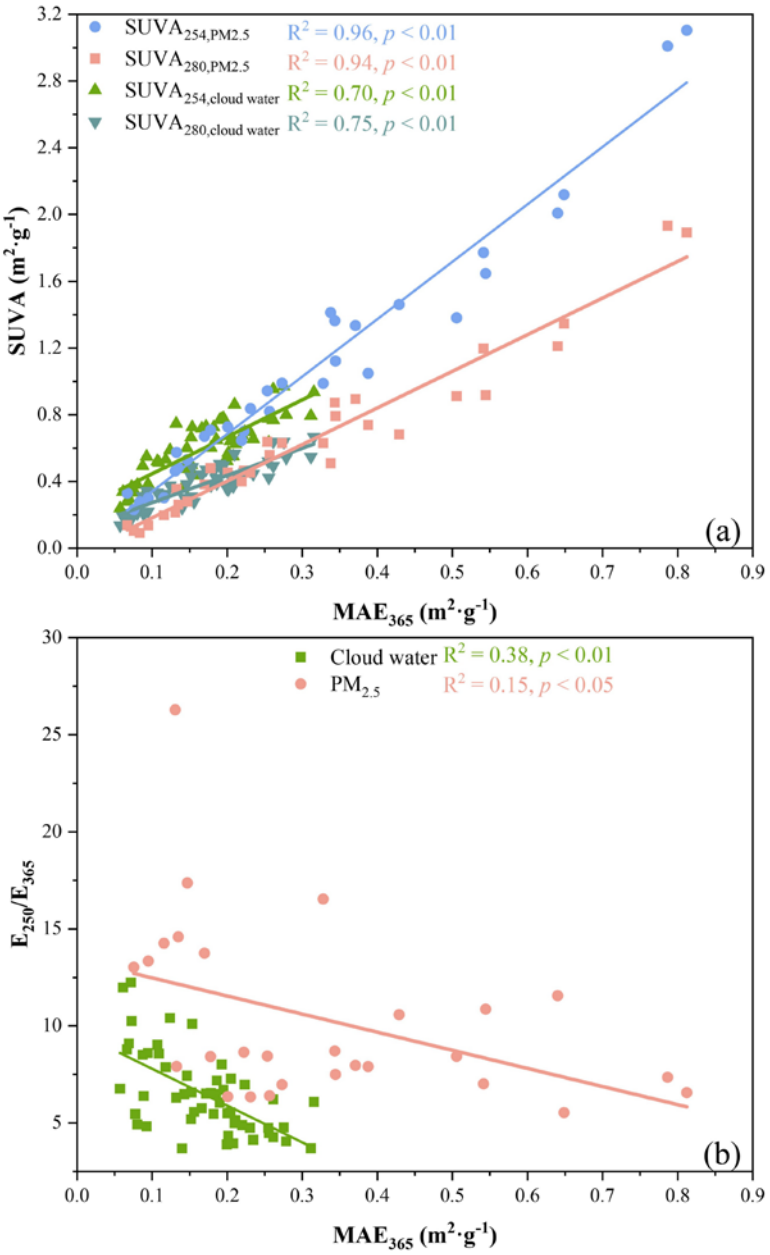

Figure S3. Correlation between MAE_{365} with SUVA (a) and E_{250}/E_{365} (b) in $PM_{2.5}$ and cloud water.

65

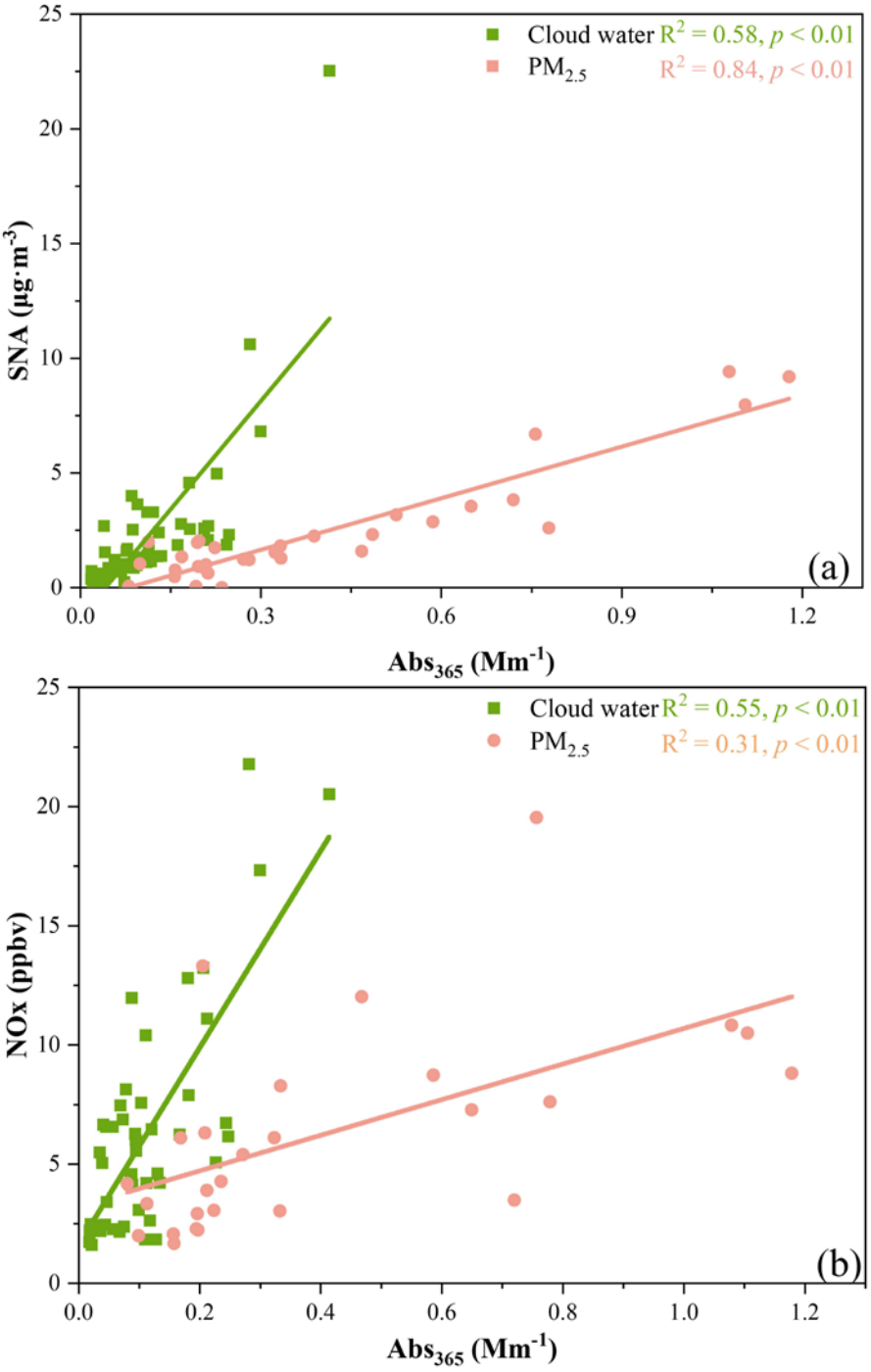

Figure S4. Correlation between Abs_{365} with SNA (a) and NOx (b) in $PM_{2.5}$ and cloud water.

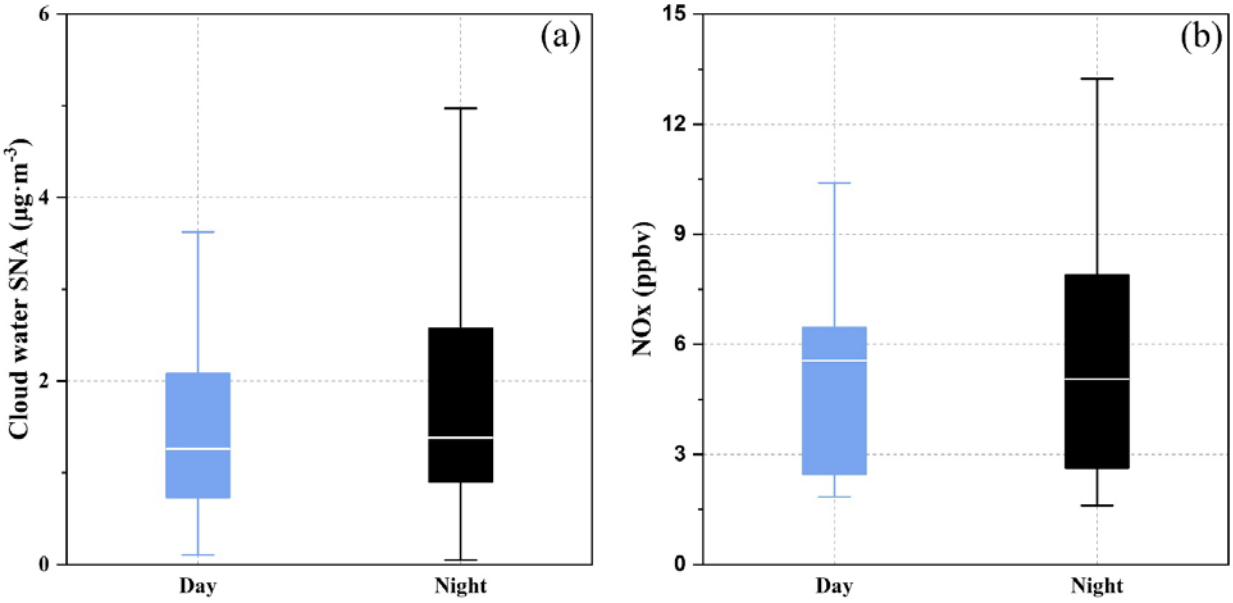

Figure S5. Diurnal variation of SNA (a) and NOx (b) in cloud water.

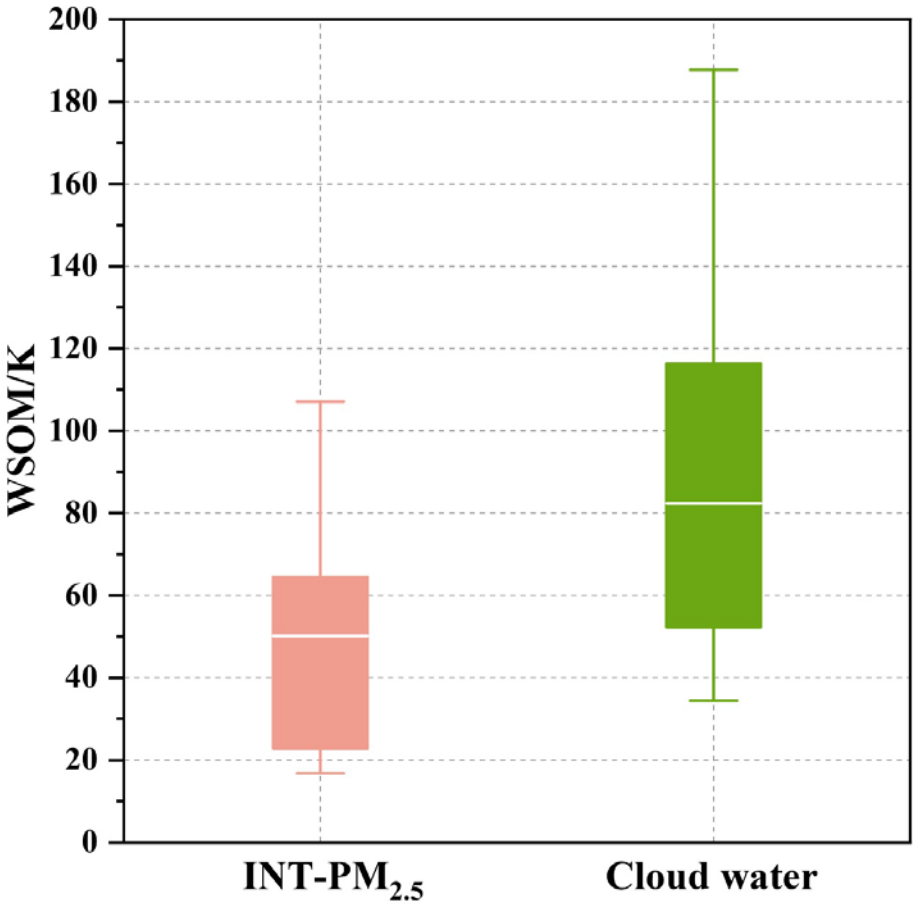

Figure S6. The WSOM/K of INT-$PM_{2.5}$ and cloud water.

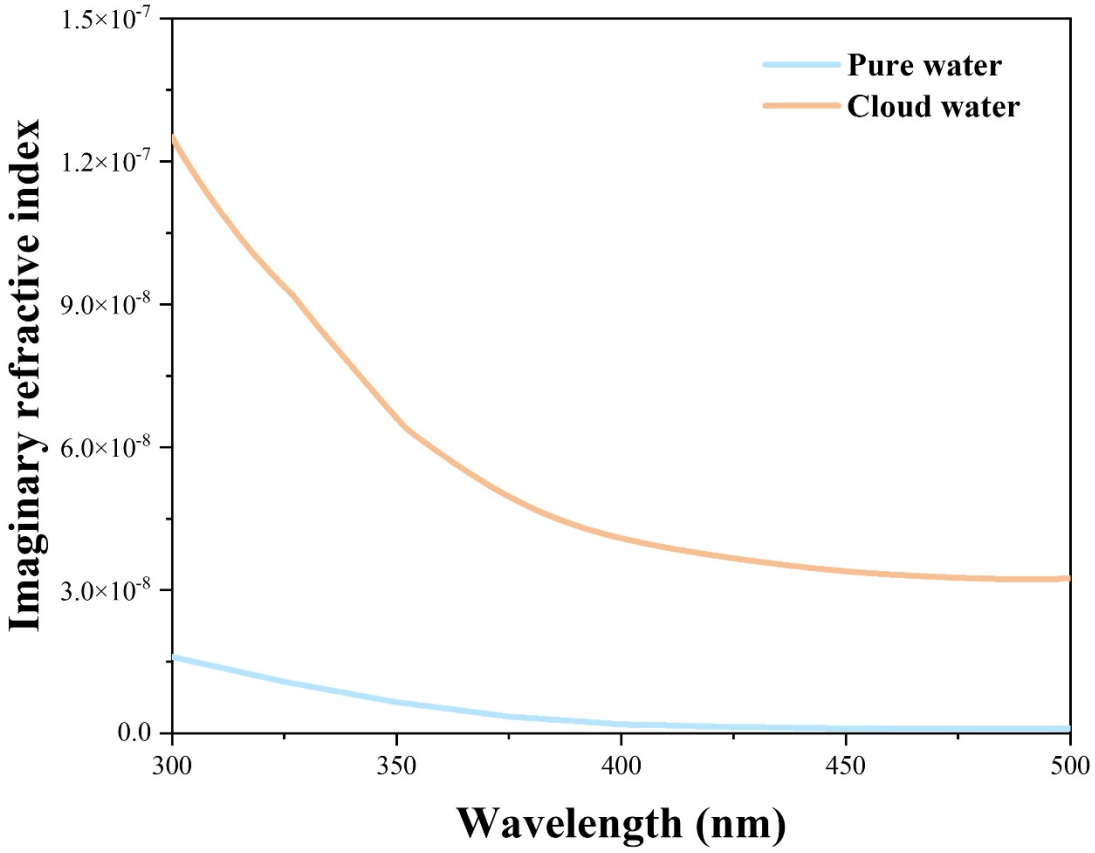

Figure S7. The imaginary refractive index of pure water and cloud water.

Table S1 The optical properties of brown carbon in different sites and sources.

Site or source	Size	Species	Abs_{365} (Mm^{-1})	MAE_{365} ($m^2 \cdot g^{-1}$)	AAE[1]	Reference
Himalayas (polluted)	PM_{10}	WSOC	0.67±1.0	0.57±0.18	4.9±0.7[A]	(Kirillova et al., 2016)
Himalayas (troposphere)	PM_{10}	WSOC	0.16±0.25	0.52±0.18	4.6±0.8[A]	(Kirillova et al., 2016)
Himalayas	PM_{10}	WSOC		0.77±0.23	5.23±0.52[B]	(Wu et al., 2019)
Xi'an	$PM_{2.5}$	WSOC	31.5±16.4	-	-	(Huang et al., 2020)
Xi'an	$PM_{2.5}$	MSOC	33.9±16.4	1.5±0.5	5.4±0.2[C]	(Huang et al., 2020)
Beijing	$PM_{2.5}$	WSOC	15.0±9.5	-	-	(Huang et al., 2020)
Beijing	$PM_{2.5}$	MSOC	26.1±18.4	1.5±0.4	5.7±0.2[C]	(Huang et al., 2020)
Nanjing	$PM_{2.5}$	WSOC	5.7	0.76	6.89[D]	(Chen et al., 2018)
Yangzhou	$PM_{2.5}$	WSOC	6.08±4.30	0.75±0.29	-	(Chen et al., 2020)
Yangzhou	$PM_{2.5}$	MSOC	13.50±7.03	1.12±0.35	-	(Chen et al., 2020)
Los Angeles	$PM_{2.5}$	WSOC	-	0.61±0.22	8.6±0.9[E]	(Soleimanian et al., 2020)
Los Angeles	$PM_{2.5}$	MSOC	-	1.35±0.89	8.3±0.9[E]	(Soleimanian et al., 2020)
Seoul	$PM_{2.5}$	WSOC	3.39±2.45	1.02-1.18	7.23±1.58[F]	(Kim et al., 2016)
Coal combustion	$PM_{2.5}$	WSOC	-	0.3-1.0	7.5-13[G]	(Li et al., 2019)
Rice straw	$PM_{2.5}$	WSOC	-	1.37±0.23	8.3±0.6[B]	(Park and Yu, 2016)
Pine needles	$PM_{2.5}$	WSOC	-	0.86±0.09	7.4±1.1[B]	(Park and Yu, 2016)
Sesame stems	$PM_{2.5}$	WSOC	-	1.38±0.21	8.0±0.8[B]	(Park and Yu, 2016)
Coal smoke	$PM_{2.5}$	WSOC	-	0.42±0.03	13.1±0.1[G]	(Fan et al., 2016)
Corn straw smoke	$PM_{2.5}$	WSOC	-	1.56±0.34	6.7±0.5[G]	(Fan et al., 2016)

[1]AAE values are calculated within the following ranges.
[A]330-500 nm, [B]300-400 nm, [C]300-500 nm, [D]300-600 nm, [E]330-550 nm, [F]300-700 nm, [G]330-400 nm.

Table S2 The secondary contribution of brown carbon identified by MRS.

Site	Size	Wavelength (nm)	Relative contribute (%)	Reference
Tibetan Plateau	$PM_{2.5}$	370-660	68-91[1]	(Wang et al., 2019a)
Athens	-	370	11[1]	(Kaskaoutis et al., 2021)
Wuhan	-	370-660	65-77[1]	(Wang et al., 2021)
Xianghe	$PM_{1.0}$	370-660	19-46[1]	(Wang et al., 2019b)
Harbin	$PM_{2.5}$	370	45.2[1]	(Zhang et al., 2021)
Beijing	$PM_{2.5}$	370	56.4[1]	(Zhang et al., 2021)
Xi'an	$PM_{2.5}$	370	32.0[1]	(Zhang et al., 2021)
Shanghai	$PM_{2.5}$	370	20.3[1]	(Zhang et al., 2021)
Wuhan	$PM_{2.5}$	370	69.4[1]	(Zhang et al., 2021)
Guangzhou	$PM_{2.5}$	370	72.2[1]	(Zhang et al., 2021)
Xi'an	-	370	48[1]	(Zhang et al., 2020)
Hongkong	-	370	76[1]	(Zhang et al., 2020)
Qinghai Lake	-	370	34[2]	(Zhu et al., 2021)
Beiluhe	-	370	16[2]	(Zhu et al., 2021)
Ngari	-	370	27[2]	(Zhu et al., 2021)
Mount Hua	$PM_{2.5}$	370-660	86-95[1]	(Gao et al., 2022)
Nanjing	$PM_{2.5}$	370-660	2-7[2]	(Lin et al., 2021)
Sanya	$PM_{2.5}$	370-660	3-5[2]	(Wang et al., 2020)

[1]The relative contribute of $Abs_{BrC,\ sec}$ to Abs_{BrC}.
[2]The relative contribute of $Abs_{BrC,\ sec}$ to total particle light-absorption.

Table S3 Q values for PMF analysis with different number of factors.

Num. of factors	$R^{2\#}$ for all input species	R^2 for WSOC	R^2 for Abs_{365}	Q_{robust}*	Q_{robust}/Q_{theory}
2	0.50-0.97	0.81	0.50	3713.9	0.88
3	**0.44-0.97**	**0.84**	**0.61**	**2508.3**	**0.92**
4	0.73-0.98	0.87	0.73	1725.9	0.93
5	0.77-0.99	0.88	0.85	1326.9	0.94

85 #R^2 between the observed and predicted species
*Q_{robust} with F_{peak}=0

Reference

Chen, Q., Miyazaki, Y., Kawamura, K., Matsumoto, K., Coburn, S., Volkamer, R., Iwamoto, Y., Kagami, S., Deng, Y., Ogawa, S., Ramasamy, S., Kato, S., Ida, A., Kajii, Y. and Mochida, M.: Characterization of Chromophoric Water-Soluble Organic Matter in Urban, Forest, and Marine Aerosols by HR-ToF-AMS Analysis and Excitation-Emission Matrix Spectroscopy, Environ. Sci. Technol., 50(19), 10351–10360, doi:10.1021/acs.est.6b01643, 2016.

Chen, Y., Ge, X., Chen, H., Xie, X., Chen, Y., Wang, J., Ye, Z., Bao, M., Zhang, Y. and Chen, M.: Seasonal light absorption properties of water-soluble brown carbon in atmospheric fine particles in Nanjing, China, Atmos. Environ., 187(June), 230–240, doi:10.1016/j.atmosenv.2018.06.002, 2018.

Chen, Y., Xie, X., Shi, Z., Li, Y., Gai, X., Wang, J., Li, H., Wu, Y., Zhao, X., Chen, M. and Ge, X.: Brown carbon in atmospheric fine particles in Yangzhou, China: Light absorption properties and source apportionment, Atmos. Res., 244(April), doi:10.1016/j.atmosres.2020.105028, 2020.

Fan, X., Wei, S., Zhu, M., Song, J. and Peng, P.: Comprehensive characterization of humic-like substances in smoke PM2.5 emitted from the combustion of biomass materials and fossil fuels, Atmos. Chem. Phys., 16(20), 13321–13340, doi:10.5194/acp-16-13321-2016, 2016.

Gao, Y., Wang, Q., Li, L., Dai, W., Yu, J., Ding, L., Li, J., Xin, B., Ran, W., Han, Y. and Cao, J.: Optical properties of mountain primary and secondary brown carbon aerosols in summertime, Sci. Total Environ., 806, doi:10.1016/j.scitotenv.2021.150570, 2022.

Gelencsér, A., Hoffer, A., Kiss, G., Tombácz, E., Kurdi, R. and Bencze, L.: In-situ formation of light-absorbing organic matter in cloud water, J. Atmos. Chem., 45(1), 25–33, doi:10.1023/A:1024060428172, 2003.

Huang, R. J., Yang, L., Shen, J., Yuan, W., Gong, Y., Guo, J., Cao, W., Duan, J., Ni, H., Zhu, C., Dai, W., Li, Y., Chen, Y., Chen, Q., Wu, Y., Zhang, R., Dusek, U., O'Dowd, C. and Hoffmann, T.: Water-Insoluble Organics Dominate Brown Carbon in Wintertime Urban Aerosol of China: Chemical Characteristics and Optical Properties, Environ. Sci. Technol., 54(13), 7836–7847, doi:10.1021/acs.est.0c01149, 2020.

Huguet, A., Vacher, L., Relexans, S., Saubusse, S., Froidefond, J. M. and Parlanti, E.: Properties of fluorescent dissolved organic matter in the Gironde Estuary, Org. Geochem., 40(6), 706–719, doi:10.1016/j.orggeochem.2009.03.002, 2009.

Kaskaoutis, D. G., Grivas, G., Stavroulas, I., Bougiatioti, A., Liakakou, E., Dumka, U. C., Gerasopoulos, E. and Mihalopoulos, N.: Apportionment of black and brown carbon spectral absorption sources in the urban environment of Athens, Greece, during winter, Sci. Total Environ., 801, 149739, doi:10.1016/j.scitotenv.2021.149739, 2021.

Kim, H., Kim, J. Y., Jin, H. C., Lee, J. Y. and Lee, S. P.: Seasonal variations in the light-absorbing properties of water-soluble and insoluble organic aerosols in Seoul, Korea, Atmos. Environ., 129, 234–242, doi:10.1016/j.atmosenv.2016.01.042, 2016.

Kirillova, E. N., Marinoni, A., Bonasoni, P., Vuillermoz, E., Facchini, M. C., Fuzzi, S. and Decesari, S.: Light absorption properties of brown carbon in the high Himalayas, J. Geophys. Res., doi:10.1002/2016JD025030, 2016.

Li, M., Fan, X., Zhu, M., Zou, C., Song, J., Wei, S., Jia, W. and Peng, P.: Abundance and Light Absorption Properties of Brown Carbon Emitted from Residential Coal Combustion in China, Environ. Sci. Technol., 53(2), 595–603, doi:10.1021/acs.est.8b05630, 2019.

Lin, Y. C., Zhang, Y. L., Xie, F., Fan, M. Y. and Liu, X.: Substantial decreases of light absorption, concentrations and relative contributions of fossil fuel to light-absorbing carbonaceous aerosols attributed to the COVID-19 lockdown in east China, Environ. Pollut., doi:10.1016/j.envpol.2021.116615, 2021.

McKnight, D. M., Boyer, E. W., Westerhoff, P. K., Doran, P. T., Kulbe, T. and Andersen, D. T.: Spectrofluorometric characterization of dissolved organic matter for indication of precursor organic material and aromaticity, Limnol. Oceanogr., doi:10.4319/lo.2001.46.1.0038, 2001.

Park, S. S. and Yu, J.: Chemical and light absorption properties of humic-like substances from biomass burning emissions under controlled combustion experiments, Atmos. Environ., doi:10.1016/j.atmosenv.2016.04.022, 2016.

Soleimanian, E., Mousavi, A., Taghvaee, S., Shafer, M. M. and Sioutas, C.: Impact of secondary and primary particulate matter (PM) sources on the enhanced light absorption by brown carbon (BrC) particles in central Los Angeles, Sci. Total Environ., 705, 135902, doi:10.1016/j.scitotenv.2019.135902, 2020.

Wang, Q., Han, Y., Ye, J., Liu, S., Pongpiachan, S., Zhang, N., Han, Y., Tian, J., Wu, C., Long, X., Zhang, Q., Zhang, W., Zhao, Z. and Cao, J.: High Contribution of Secondary Brown Carbon to Aerosol Light Absorption in the Southeastern Margin of Tibetan Plateau, Geophys. Res. Lett., 46(9), 4962–4970, doi:10.1029/2019GL082731, 2019a.

Wang, Q., Ye, J., Wang, Y., Zhang, T., Ran, W., Wu, Y., Tian, J., Li, L., Zhou, Y., Hang Ho, S. S., Dang, B., Zhang, Q., Zhang, R., Chen, Y., Zhu, C. and Cao, J.: Wintertime Optical Properties of Primary and Secondary Brown Carbon at a Regional Site in the North China Plain, Environ. Sci. Technol., 53(21), 12389–12397, doi:10.1021/acs.est.9b03406, 2019b.

Wang, Q., Liu, H., Wang, P., Dai, W., Zhang, T., Zhao, Y., Tian, J., Zhang, W., Han, Y. and Cao, J.: Optical source apportionment and radiative effect of light-absorbing carbonaceous aerosols in a tropical marine monsoon climate zone: The importance of ship emissions, Atmos. Chem. Phys., 20(24), 15537–15549, doi:10.5194/acp-20-15537-2020, 2020.

Wang, Q., Wang, L., Tao, M., Chen, N., Lei, Y., Sun, Y., Xin, J., Li, T., Zhou, J., Liu, J., Ji, D. and Wang, Y.: Exploring the variation of black and brown carbon during COVID-19 lockdown in megacity Wuhan and its surrounding cities, China, Sci. Total Environ., 791, 148226, doi:10.1016/j.scitotenv.2021.148226, 2021.

Wu, G., Ram, K., Fu, P., Wang, W., Zhang, Y., Liu, X., Stone, E. A., Pradhan, B. B., Dangol, P. M., Panday, A. K., Wan, X., Bai, Z., Kang, S., Zhang, Q. and Cong, Z.: Water-Soluble Brown Carbon in Atmospheric Aerosols from Godavari (Nepal), a Regional Representative of South Asia, Environ. Sci. Technol., 53(7), 3471–3479, doi:10.1021/acs.est.9b00596, 2019.

Zhang, Q., Shen, Z., Zhang, L., Zeng, Y., Ning, Z., Zhang, T., Lei, Y., Wang, Q., Li, G., Sun, J., Westerdahl, D., Xu, H. and Cao, J.: Investigation of Primary and Secondary Particulate Brown Carbon in Two Chinese Cities of Xi'an and Hong Kong in Wintertime, Environ. Sci. Technol., 54(7), 3803–3813, doi:10.1021/acs.est.9b05332, 2020.

Zhang, Q., Shen, Z., Zhang, T., Kong, S., Lei, Y., Wang, Q., Tao, J., Zhang, R., Wei, P., Wei, C., Cui, S., Cheng, T., Ho, S. S. H., Li, Z., Xu, H. and Cao, J.: Spatial distribution and sources of winter black carbon and brown carbon in six Chinese megacities, Sci. Total Environ., doi:10.1016/j.scitotenv.2020.143075, 2021.

Zhu, C. S., Qu, Y., Huang, H., Chen, J., Dai, W. T., Huang, R. J. and Cao, J. J.: Black Carbon and Secondary Brown Carbon, the Dominant Light Absorption and Direct Radiative Forcing Contributors of the Atmospheric Aerosols Over the Tibetan Plateau, Geophys. Res. Lett., 48(11), 1–9, doi:10.1029/2021GL092524, 2021.

Zsolnay, A., Baigar, E., Jimenez, M., Steinweg, B. and Saccomandi, F.: Differentiating with fluorescence spectroscopy the sources of dissolved organic matter in soils subjected to drying, Chemosphere, doi:10.1016/S0045-6535(98)00166-0, 1999.